



Embryonic development of the tropical bivalve *Tivela mactroides* (Born, 1778) (Veneridae: subfamily Meretricinae): a SEM study

Thomas SILBERFELD and Olivier GROS*

UMR 7138 Systématique-Adaptation-Evolution, équipe Symbiose
Université des Antilles et de la Guyane, U.F.R des Sciences Exactes et Naturelles.
Département de Biologie. 97159 Pointe-à-Pitre Cedex, Guadeloupe (France).

*Corresponding author: Tel 590 48 92 13, Fax: 590 48 92 19, E-mail olivier.gros@univ-ag.fr

Abstract: The embryonic development of *Tivela mactroides*, from fertilization to straight-hinge veliger D-stage larva occurs in 18 hours at 25°C. Scanning electronic observations show that morphogenetic processes result in a gastrula with two depressions 4 hours after fertilization ($T_0 + 4h$). Two hours later, one depression, located at the animal pole, develops into an open cave, the floor of which becomes the shell field located below the lower face of the prototrochal pad. The invagination located at the vegetal pole features the blastopore. At $T_0 + 6h$, the late gastrula has differentiated into a typical motile trochophore with a shell field synthesizing the organic part of the shell. At $T_0 + 8h$, the shell field, located between the prototroch and the telotroch, appears as a saddle-shaped region with a wrinkled surface extending on both sides of the embryo, establishing bilateral symmetry. At $T_0 + 12h$, the prototroch slides toward the anterior region by outgrowth of the shell material. At $T_0 + 18h$, the prodissoconch I formation is completed and the D-stage larvae possess a calcified shell. At this stage of development, the functional velum is composed of four bands of cilia. Our observations seem to confirm the interpretation of shell differentiation proposed recently by Mouëza et al. (2006) for bivalves even if Transmission Electronic observations will be necessary to validate definitively such a model in the Meretricinae sub-family.

Resumé : Développement embryonnaire du bivalve tropical *Tivela mactroides* (Born, 1778) (Veneridae : Meretricinae) : une étude en microscopie électronique à balayage. Le développement embryonnaire de *Tivela mactroides*, de la fécondation au stade larve D se déroule en 18 heures à 25°C. Les observations en microscopie électronique à balayage montrent que les processus morphogénétiques aboutissent 4 heures après fécondation ($T_0 + 4h$) à une gastrula pourvue de deux dépressions : celle située au pôle animal se développe en une large cavité dont seul le plancher, situé sous le bourrelet prototrochal, correspond à la région coquillière, l'invagination du pôle végétatif représentant le blastopore. À $T_0 + 6h$, la gastrula s'est différenciée en une trochophore mobile avec une région coquillière synthétisant la coquille embryonnaire. À $T_0 + 8h$, la région coquillière, d'aspect fripé, prend une forme en haltère qui, en se développant de chaque côté de l'embryon, établit la symétrie bilatérale. À $T_0 + 12h$, la prototroche est déplacée vers la région antérieure suite à l'expansion de la coquille. À $T_0 + 18h$, la formation de la prodissoconque I est terminée et la larve D possède une coquille calcifiée. Cette larve véligère possède un velum fonctionnel constitué de quatre bandes de cils. Nos observations semblent confirmer

le modèle de différenciation de la coquille proposé par Mouëza et al. (2006) pour les bivalves, cependant des observations en microscopie électronique seraient nécessaires pour valider définitivement un tel modèle dans la sous-famille des Meretricinae.

Keywords: Mollusca • Bivalvia • Ontogenesis • SEM

Introduction

Embryonic, larval and post-larval development of bivalves has long been studied with a view to elaborate an aquaculture of species with economic interest, to identify the systematic location of species at larval planktonic stages, or to understand ontogenesis processes occurring specifically in this invertebrate embranchment. In Eulamellibranchia, larval development has been first described in a number of species with as much details as possible using light microscopy (Loosanoff & Davis, 1963; Loosanoff et al., 1966; Frenkiel & Mouëza, 1979; Sastry, 1979). More recently, some papers were published about the embryonic development of bivalves with scanning electron microscopy (SEM) analysis, such as those on pectinids (Hodgson & Burke, 1988; Bellolio et al., 1993), lucinids (Gros et al., 1997 & 1999), on a venerid (Mouëza et al., 1999), and on a nuculid (Zardus & Morse, 1998). Few papers have combined TEM and SEM analysis as those of Eyster & Morse (1984) on *Spisula solidissima*, Casse et al. (1998) on *Pecten maximus*, Zardus & Morse (1998) on *Acila castrensis*, and Mouëza et al. (2006) on the venerid *Chione cancellata*. These last authors have even proposed a new model to explain the shell formation and differentiation in bivalves (Mouëza et al., 2006). In order to confirm such model, we have checked embryonic development and shell-field differentiation in a new investigated bivalve sub-family.

Moreover, the embryonic development of *T. mactroides* will allow an ontogenetic comparison with the other species of venerid bivalves already described. Indeed, Ansell (1962) pointed that the study of developmental stages of members of the family Veneridae was particularly relevant, while this family is considered as a crown group within the Eulamellibranchia Molluscs (Giribet & Wheeler, 2002).

The purpose of the present paper is (i) to describe the whole embryonic development in a Meretricinid species, (ii) to compare patterns of embryonic development in tropical venerids, and (iii) to investigate selected aspects of ontogenesis in this family in order to confirm the new shell differentiation model recently suggested in bivalves by Mouëza et al. (2006).

Materials and methods

Individual collection

Tivela mactroides BORN 1778 is a large clam (up to 45 mm in shell length) belonging to the family Veneridae (subfamily Meretricinae), distributed from West Indies to Brazil (Warmke & Abbott, 1962; Abbott, 1974). It lives shallowly burrowed in the sandy bottoms of the Guadeloupe coast where it is widely collected and consumed under the vernacular name of "Chaudron". Adult specimens of *T. mactroides* were collected by hand in June 2004 in shallow sandy bottoms of "La Source" beach in Guadeloupe (Fig. 1).

Spawning and fertilization

Adults of *T. mactroides* can spawn throughout the year in the field depending to environmental stresses (personal observation). For each spawning assay, 20-30 freshly collected individuals were used. Specimens were carefully cleaned by scrubbing their shell, and placed in a 50-litre tank filled with seawater, until the onset of spawning. Various stimulations as osmotic stress (individuals were placed in fresh water up to 15 minutes), one-hour exundation on a sunny place, and serotonin injections were used to induce spawning. Once spawning was completed, adults were taken out. The density of the embryos was adjusted to 30.000 per litre. The water was then softly bubbled directly in the spawning tank, in order to avoid sedimentation of eggs and embryos and also hypoxia due to the high oxygen consumption by the embryos themselves. Development was proceeded at room temperature, i.e. 25°C, at a salinity of 36 ± 1 which is typical for their natural habitat. No antibiotics were used and all seawater used for fertilization and rearing was filtered through a 5- μ m Millipore cartridge filter.

Sampling and fixation

To study the successive embryonic stages of *T. mactroides*, 500 mL of seawater containing 4-5 thousands of embryos were sampled on a 26- μ m mesh nylon screen every hour

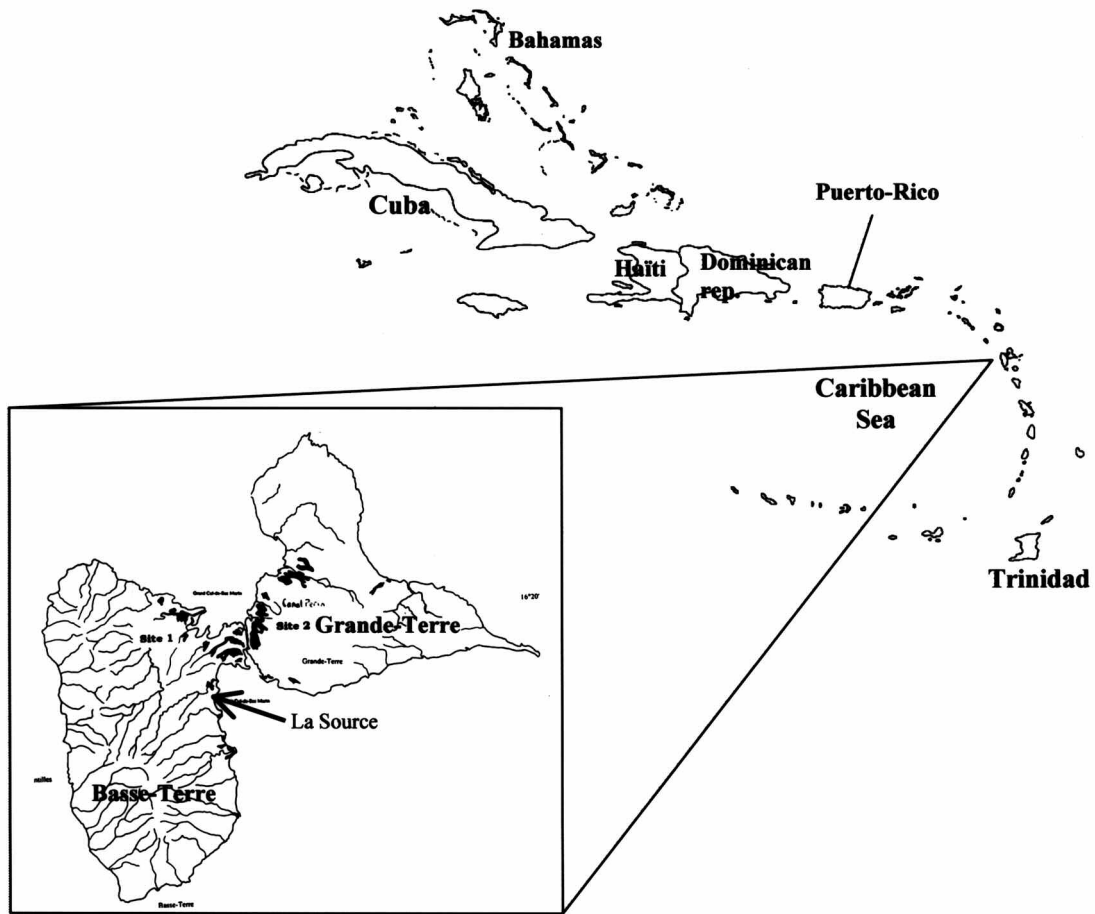


Figure 1. Map of Guadeloupe showing the location of the site of bivalve collection: *La Source*.

Figure 1. Carte de la Guadeloupe indiquant la localisation du site de *la Source*.

throughout the entire embryonic development (i.e. ~ 20 hours). The embryos were then placed in a small basket for a safe handling and transferred into a fixative solution of 2% glutaraldehyde in filtered seawater at 4°C for at least 2 hours before dehydration.

The first D-shaped larval stages have required a previous specific treatment, in order to avoid the retraction of velum inside the calcified valves when glutaraldehyde is added. The simplest way to do that was to put larvae in a small volume of seawater at -20 °C for 5 minutes, so that most of the larvae could not retract their velum (frozen anaesthetized-like) when pouring the fixative solution.

SEM preparation

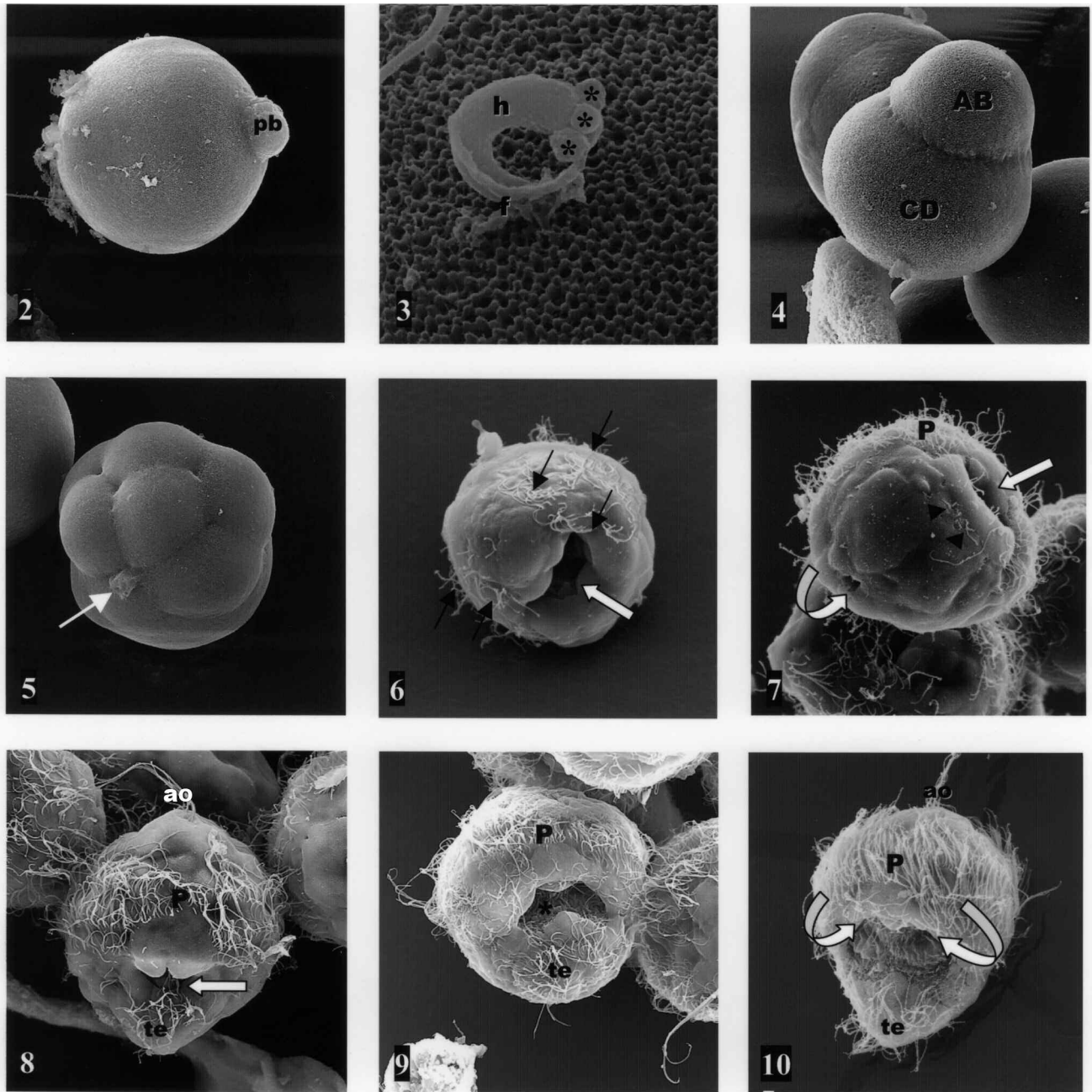
After the fixation, embryos were twice rinsed in 0.1 M cacodylate buffer adjusted to pH 7.2 and 1000 mOsM, then dehydrated through a graded acetone series, before drying by CO₂ at critical point in a Biorad apparatus (Polaron, Critical Point Drier). Then samples were sputter-coated

with gold (Sputter Coater SC500, Biorad) before observation in a SEM Hitachi S-2500 at a 20 kV accelerating tension.

Results

Spawn induction

Adult individuals of *Tivela mactroides* spawned in the hatchery throughout the year as observed in their natural environment (personal observations). In bivalves, spawning can be induced by applying a stress of various nature (for review, see Mouëza et al., 1999). According to Matsutani & Nomura (1982) and Gibbons & Castagna (1984), a chemical stress has been applied, by injection of a 2 mM serotonin solution in 0.22 µm filtered seawater in the visceral mass. But *T. mactroides* did not seem to be susceptible to this chemical stimulus. Therefore, other kinds of stress were tested such as osmotic stress by putting the



clams into freshwater at room temperature for 15 minutes followed, or not, by a one-hour exundation step on a sunny place. This last method has been successful. We usually observed a spawning of male and female gametes within 30 minutes after putting back the individuals in a new tank.

Fertilization

Oocytes are spherical, 55-60 μm diameter cells (Fig. 2). They have a thin vitelline coat and no prominent jelly coat. The sperm is particularly motile. It is characterized by a short curved head, 5- μm long head, and by a flagellum

about 50- μm long. The middle piece appears made of four spherical mitochondria (Fig. 3). Fertilization normally occurs and no polyspermy was observed in the several batches obtained during this study. The appearance of the first polar body (Fig. 2) 10 to 15 minutes after fertilization ($T_0 + 15 \text{ min}$) is a visual witness of a managed fertilization.

Embryonic shell development

The first segmentation cleavage occurs within one hour after fertilization and results in two unequal blastomeres



Figures 2-10. *Tivela mactroides*. SEM view from egg to young trochophore. **2.** Fertilized egg. The first polar body (pb) is located on the opposite position of the sperm entrance indicating the animal pole of the spawned egg. (x 1500). **3.** Sperm lying on the surface of an egg; short, arched head (h) and a middle piece composed of four mitochondria (asterisks). On this view, the flagellum (f) appears broken (x 20000). **4.** Two-cell embryo with unequal blastomeres AB and CD. The polar body, which is in the cleavage plane, does not appear (x 1500). **5.** Young morula 2.5 to 3 hours after fertilization. The polar body is indicated by an arrow. (x 1500). **6.** The early gastrula differentiated at $T_0 + 4h$ is characterized by a large depression (white arrow) in its vegetal pole. Its circular margin is surrounded by cilia (arrows) (x 1500). **7.** Gastrulae between $T_0 + 4h$ and $T_0 + 5h$. At this stage of development, the difference between the diameters of the blastopore (curved arrow) and the other depression (arrow) is obvious. The first cilia (arrow heads) of the future telotroch are differentiated in the posterior region. P: prototroch (x 1500). **8.** Early trochophore around $T_0 + 7h$. The apical sense organ (ao) located in the middle of the apical plate is surrounded by the prototroch (P). Below such structure, there is the large open cave (arrow) representing the shell field whose floor is smooth. The telotroch (te) appears now well developed with numerous cilia (x 1500). **9.** Dorsal view of an early trochophore at $T_0 + 8h$. The floor of the open cave, located in the dorsal side of the trochophore, differentiates a wrinkled aspect (asterisk) on its surface. Such aspect indicates the synthesis of the first organic material in the shell field. P: prototroch; te: telotroch (x 1500). **10.** One hour later, the wrinkled shell organic material is dumbbell shaped at $T_0 + 9h$. ao: apical sense organ; curved arrows: prototrochal pad; P: prototroch; te: telotroch (x 1500).

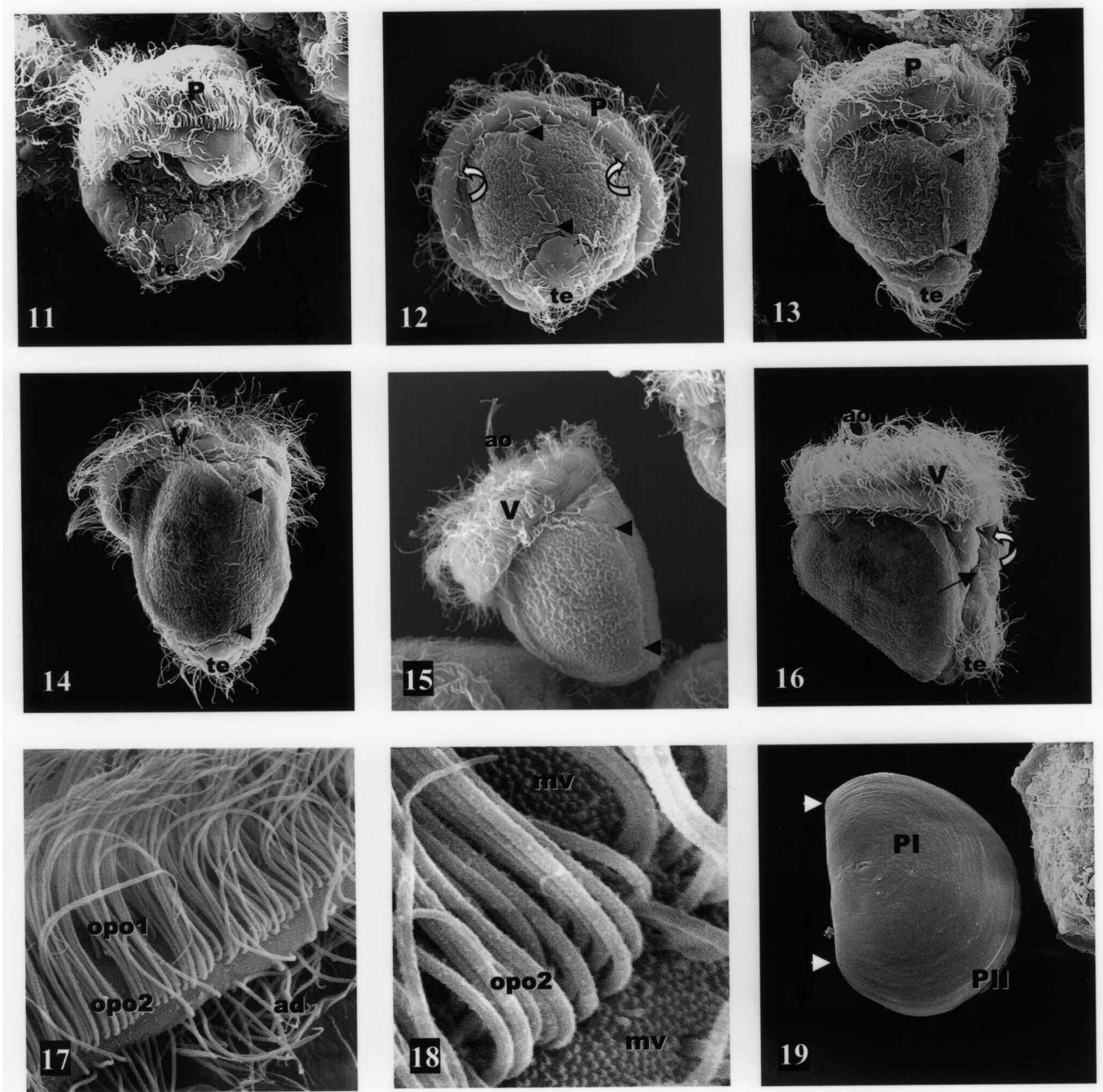
Figures 2-10. *Tivela mactroides*. Vues en Microscopie Electronique à Balayage du développement embryonnaire : de l'œuf à la jeune trochophore. **2.** Oeuf fécondé. Le premier globule polaire (pb) se situe à l'opposé du point d'entrée du spermatozoïde, indiquant ainsi le pôle animal de l'œuf fécondé (x 1500). **3.** Spermatozoïde observé en surface d'un ovocyte. Il possède une tête courte (h) et une pièce intermédiaire composée de 4 mitochondries (astérisques). Sur cette vue, le flagelle est cassé (f) (x 20000). **4.** Embryon au stade 2 cellules avec deux blastomères inégaux AB et CD. Le globule polaire, qui est normalement dans le plan de division, n'est pas visible sur la photo (x 1500). **5.** Jeune morula 2,5 à 3 heures après fécondation ($T_0 + 3h$). Le globule polaire est indiqué par une flèche (x 1500). **6.** La jeune gastrula différenciée à $T_0 + 4h$ est caractérisée par une large dépression (flèche blanche) au pôle végétatif dont le pourtour est entouré de cils (flèches) (x 1500). **7.** Gastrula entre $T_0 + 4h$ et $T_0 + 5h$. A ce stade de développement, la différence de diamètre entre le blastopore (flèche courbe) et l'autre dépression (flèche) est évidente. Les premiers cils de la future télotroche se différencient dans la région postérieure. P: prototroche (x 1500). **8.** Jeune trochophore vers $T_0 + 7h$. L'organe sensoriel apical (ao) situé au milieu du plateau apical est entouré par la prototroche (P). Sous cette dernière se trouve la large dépression représentant la région coquillière (flèche) dont le plancher est d'aspect lisse. La télotroche (te) semble maintenant bien développée avec de nombreux cils (x 1500). **9.** Vue dorsale d'une jeune trochophore à $T_0 + 8h$. Le plancher de cette "caverne" localisée sur la face dorsale de la trochophore, possède une surface d'aspect fripé (astérisque). C'est à cet endroit qu'a lieu la synthèse organique de la coquille embryonnaire. P: prototroche; te: télotroche (x 1500). **10.** Une heure plus tard, la pellicule coquillière d'aspect fripé commence à prendre la forme d'une haltère à $T_0 + 9h$. Les flèches courbes indiquent les bourrelets prototrochaux. ao: organe apical; P: prototroche; te: télotroche (x 1500).

conventionally named AB and CD (Fig. 4) without polar lobe. The second and third segmentation cleavages occur between $T_0 + 1h$ and $T_0 + 2h$. The second cleavage, unequal and whose axis is orthogonal to the former, results in three equal A-, B-, C-blastomeres and a larger D-blastomere (not shown). Polar bodies are located at the intersection of the planes of cleavage. Then, successive cleavages, with a spiral pattern, result within the third hour of development in a morula (Fig. 5), which quickly develops into a non-ciliated blastula.

The early gastrula stage is detected between $T_0 + 3h$ and $T_0 + 4h$. Young gastrulae are characterized by the apparition of two cellular depressions located in the vegetative hemisphere: the ventral one features the blastopore, whereas the larger one featuring the shell-field occurs dorsally to the other (Fig. 6). Thus, there are two independent structures with distinctive functions in gastrulae (Fig. 7).

From the fourth hour of development, some scarce cilia begin to cover the anterior region of the embryo prefiguring the future prototroch (Figs 6-7). Consequently, such embryos begin to rotate moving in the water column. The morphogenetic movements result dorsally in a wide open shell field depression, whereas the diameter of the blastopore goes on decreasing (Fig. 7).

At $T_0 + 5h$, the difference between the diameters of the two depressions becomes obvious (Fig. 7). The dorsal region is marked by an open cave, which is expanding under and posterior to the developing prototrochal pad (Fig. 7). At $T_0 + 7h$, the cilia of the coming telotroch begin to appear on the posterior area of the embryo while the first cilia of the apical sense organ typical of young trochophores appear (Fig. 8). At $T_0 + 8h$, the shell field depression elongates transversally in a dorsal slit (Fig. 9). A wrinkled material was observed on the floor of the larger



depression (Fig. 9), the roof of this depression featuring the lower part of the pad of the prototroch. This wrinkled material features the organic material secreted by specialized cells of the periostracum.

Between $T_0 + 9h$ and $T_0 + 10h$, the late gastrula has differentiated into a typical motile trochophore (Figs 10 & 11) which exhibits a well developed prototroch composed of two ciliary crowns delimiting two regions : (i) the anterior pretrochal area bearing the long ciliary tuft of the apical sense organ, and (ii) the posterior post-trochal area with the blastopore in a ventral position and the shell field

in a dorsal position. The latter is bordered on its posterior margin by the developing telotroch (Figs 10 & 11). The number of sensorial cilia of the apical sense organ progressively increases; their bases are free whereas they are stuck all along their length (not shown).

At $T_0 + 11h$, the shell field continues to evaginate; the shell pellicle is constituted by two uncalcified lobes of wrinkled aspect, surrounded by an ectodermal pad (Fig. 12). The dorsal extension of the shell field (epiboly) results in a slide of the ventral blastopore in direction of the anterior part of the trochophore.



Figures 11-19. *Tivela mactroides*. SEM views from young trochophore to D-larva veliger. **11.** Dorsal view. Beginning of the saddle stage in a 10-hour trochophore. The shell field keeps on extending over the dorsal area of the embryo. The bilateral symmetry appears in the shell field area. P: prototroch; te: telotroch (x 1500). **12.** A trochophore in a dorsal view between $T_0 + 10h$ and $T_0 + 11h$. The expansion of the shell begins to laterally compress the body of the trochophore pushing aside the prototrochal pads (curved arrows). The hinge line, which is now obvious, is delineated by arrow heads. P: prototroch; te: telotroch (x 1500). **13.** Between $T_0 + 11h$ and $T_0 + 12h$, the lateral compression of the trochophore is obvious. The hinge line is delineated by arrow heads. P: prototroch; te: telotroch (x 1100). **14.** Dorsal view of a 12-hour old trochophore. The hinge line is clearly delineated (arrow heads). te: telotroch; V: velum (x 1100). **15.** Lateral view of a trochophore at $T_0 + 12h$. The valves, while covering the whole body and laterally compressing the trochophore, still appear uncalcified as suggested by their wrinkled aspect. The velum (V) is now well developed. The hinge is delineated by arrow heads. ao: apical sense organ (x 1100). **16.** Latero-ventral view of late trochophore at $T_0 + 15h$. The first cilia of the postoral tuft (arrow) of the cilia can be observed below the mouth (curved arrow). ao: apical sense organ; te: cilia from telotroch; V: velum (x 1100). **17.** Higher magnification of the velum at $T_0 + 15h$ showing the adoral band characterized by short and randomly organized cilia (ad). The double row of the outer preoral band of the velar crown is composed of two distinct rows of independent cirri (opo1, opo2) (x 5000). **18.** Detail of the external row (opo2) of the outer preoral band in a veliger at $T_0 + 15h$. This row, as the internal one, is constituted by cirri composed of 4 to 6 cilia. mv: microvilli (x 21700). **19.** 18-hour D-larva. straight hinge is delineated by arrow heads. PI: embryonic shell; PII: larval shell. The boundary between embryonic (PI) and larval (PII) shell has already appeared; the embryonic development is done (x 1000).

Figures 11-19. *Tivela mactroides*. Vues en Microscopie Electronique à Balayage du développement embryonnaire : de la jeune trochophore à la larve D. **11.** Vue dorsale. Début du stade en haltère chez une trochophore âgée de 10 heures. La région coquillière continue de s'étendre sur la partie dorsale de l'embryon. La symétrie bilatérale au niveau de la région coquillière commence à être visible. P: prototroche; te: télotroche (x 1500). **12.** Une trochophore en vue dorsale entre $T_0 + 10h$ et $T_0 + 11h$. L'expansion de la région coquillière commence à comprimer latéralement le corps poussant en avant les bourrelets prototrochaux (flèches courbes). La charnière, qui est maintenant évidente, est délimitée par des têtes de flèche. P: prototroche; te: télotroche (x 1500). **13.** Entre $T_0 + 11h$ et $T_0 + 12h$, la compression latérale de la trochophore est bien prononcée. La charnière est délimitée par des têtes de flèche. P: prototroche ; te: télotroche (x 1300). **14.** Vue dorsale d'une trochophore âgée de 12 heures. La charnière est délimitée par des têtes de flèche. Les valves, d'aspect fripé, englobent la quasi-totalité du corps mou de l'embryon. te: télotroche; V: velum (x 1100). **15.** Vue latérale d'une trochophore à $T_0 + 12h$. Les valves, bien que recouvrant entièrement le corps de l'embryon le comprimant latéralement, semblent toujours non calcifiées d'après leur aspect fripé. Le velum (V) est maintenant bien développé. La charnière est délimitée par des têtes de flèche. ao: organe apical (x 1100). **16.** Vue latéro-ventrale d'une vieille trochophore à $T_0 + 15h$. Les premiers cils de la touffe post-orale (flèche) sont maintenant visibles sous la bouche (flèche courbe). ao: organe apical; te: cils de la télotroche; V: velum (x 1100). **17.** Fort grossissement du velum à $T_0 + 15h$ montrant la bande adorale caractérisée par des cils courts et non organisés (ad). La double rangée de cils de la bande préorale externe de la couronne vélaire est constituée de deux rangées distinctes de cirri indépendants (opo1, opo2) (x 5000). **18.** Détail de la rangée externe (opo2) de la bande préorale externe chez une jeune véligère à $T_0 + 15h$. Cette rangée, comme la rangée interne, est constituée de 4 à 6 cils par cirrus. mv: microvilli (x 21700). **19.** Larve D âgée de 18 heures. La charnière est délimitée par des flèches PI: prodissoconque I; PII : prodissoconque II. La limite entre coquille embryonnaire (PI) et coquille larvaire (PII) est bien nette. Le développement embryonnaire est terminé (x 1,000).

Between $T_0 + 10h$ and $T_0 + 12h$, the shell pellicle goes on extending anteriorly (Figs 12 & 13). The two lobes of the shell pellicle appear connected by an obvious axial line, featuring the coming hinge (Fig. 13). Moreover, the extension of the shell pellicle results in a lateral compression of the body of the larva, which is progressively covered by the lobes of the shell pellicle (Figs 13 & 14). Finally, the prototroch and the pretrochal area ventrally slide, not far from the blastopore, which features the mouth of the coming veliger larva (Fig. 16).

From $T_0 + 12h$ to $T_0 + 15h$, the valves of the shell pellicle continue to compress laterally the body of the larva (Figs 14 & 16). At $T_0 + 15h$, the prototroch now appears totally pushed aside in ventral direction, near the mouth

(Fig. 16). Moreover, it takes the shape of a prominent annular, ciliated pad: the velum (Figs 17 & 18).

At $T_0 + 15h$, the valves of the periostracum appear D-shaped with a straight hinge, which characterizes the early veliger stage in bivalves. The velum now exhibits a dense, well structured ciliary structure, with four ciliated bands (Figs 17 & 18). From the front to the posterior part of the velum, there are one outer preoral band composed of two lines of parallel cilia clustered in cirri of 4-5 stuck cilia (Fig. 18); one adoral band, on the edge of the velum, with a few non-oriented cilia; and one postoral band, whose scarce cilia posteriorly surround the mouth.

At $T_0 + 18h$, the valves appear calcified according to their smooth aspect in SEM (Fig. 19). The hinge of the D-

larva appears straight, and about 90 μm long. The antero-posterior length of the prodissoconch I is about 120 μm , and its dorso-ventral length, 80 μm . Therefore, throughout the 18 hours of development, the size of the organism has doubled.

Then, D-larvae follow their development quickly after hatching. Larval growth is characterized by the appearance of a newly secreted larval shell (prodissoconch II) in the margin of the embryonic prodissoconch I (Fig. 19).

Discussion

The embryonic stages of *Tivela mactroides* have a more or less similar development compared to the previously analyzed venerids *Anomalocardia brasiliiana* (Mouëza et al., 1999), *Chione cancellata* (Mouëza et al., 2006), and *Pitar albida* (Meuret, personal communication), although slightly faster. Gastrulae are obtained 3-4 hours after fertilization, typical trochophores 3 hours later, and fully developed veligers by 18 hours at 25°C while it takes around 24 hours at 25°C for *A. brasiliiana* and *C. cancellata*.

During gastrulation, the cave in which the shell field will develop appears before the formation of a well developed prototroch as previously described in other venerids (Mouëza et al., 1999 & 2006). These authors do not agree on the order of appearance of these two structures reviewed by Waller (1981); in this study a sequential sampling at hourly intervals confirms that, at least in small tropical venerids, this cave appears when the gastrula possesses only few cilia (Mouëza et al., 1999 & 2006).

Shell differentiation

Other authors working on shell differentiation during the embryonic development of bivalve Molluscs have reported the invagination process described one century ago by Stepanoff in Kniprath (1980). It has been suggested that the invagination either needs to close completely as in the case of *Mytilus galloprovincialis* (Kniprath, 1980) and *Pecten maximus* (Casse et al., 1998) before the shell formation, or partially, as proposed for *Spisula solidissima* (Eyster & Morse, 1984). These studies related to bivalves were based on a process described from gastropods (Kniprath, 1980; Eyster, 1983). Observations at an ultrastructural level (using both TEM and SEM) during embryonic development of *C. cancellata* lead Mouëza et al. (2006) to suggest an alternative interpretation of shell differentiation. Thus, in this new model there is no invagination of the shell field followed by an evagination as currently admitted before. The shell field only corresponds to the floor of the large depression originally located in the vegetal pole of the embryo before to be displaced to the dorsal side during the gastrulation process (Mouëza et al., 2006). Such study has

also shown that the shell field, including both shell and ligament secretory cells, does not migrate inwards and never builds an invagination by itself.

Excepted the blastopore, no additional invagination has been observed in embryos of *T. mactroides*. A large depression, which does not correspond to an invagination, has been observed in the dorsal region of the embryo with a similar development as those previously described in *A. brasiliiana* (Mouëza et al., 1999) and *C. cancellata* (Mouëza et al., 2006). Only the floor of such depression could be considered as shell field due to the presence of organic material only on one side of the depression. There is no invagination of the shell field, followed by an evagination process, in *T. mactroides*. Moreover, the SEM observations presented here confirm the fact that the new shell material spreads out, pushing the adjacent tissues as growth proceeds, overlapping the embryo, pushing aside the prototrochal pad to the top and to the front, and the telotroch to the bottom and to the front of the trochophore. Mantle epiboly and shell expansion play a major role in the transformation from trochophore to veliger by compressing the soft body and displacing the prototroch that becomes the velum. Such process was also observed on the Mactridae *Mulinia portoricensis* (personal observations).

Moreover, biomineralization analyses on embryos of *T. mactroides* have shown that aragonite appears 15 hours after fertilization while valves almost enclose the soft part of the old trochophore (unpublished data). Thus, the wrinkled aspect of the shell field is due to organic material that will become calcified at the end of the embryonic development few hours before the D-larva stage. Such phenomenon was also observed in *C. cancellata* in which different phases of mineral fraction, determined by X-ray diffraction analysis (Medaković, personal communication), were confirmed by TEM observations of aragonite crystals between the mantle and the periostracum more than 15 hours after fertilization (Mouëza et al., 2006).

In this study, we described the outer preoral bands constituted by long cirri composed of 5-7 cilia separated by a narrow space as described in *A. brasiliiana* for 3 day-old veligers according to SEM views (Mouëza et al., 1999) or in *C. cancellata* according to TEM views (Mouëza et al., 2006). However, it is difficult to confirm that the velum of *T. mactroides* 18h-old veligers possesses an inner preoral band as described in 3 day-old veligers of *A. brasiliiana* (Mouëza et al., 1999). All other bands constituting the velum are similarly organized.

Moreover, an accurate description of the entire developmental stages of *T. mactroides* during the larval and post-larval development could be useful in the future with a view to use this venerid species as a candidate for the development of mariculture of native species as a part of a Caribbean aquaculture.

References

- Abbott R.T. 1974.** American seashells. Van Nostrand Reinhold Company. 663 pp
- Ansell A.D. 1962.** The functional morphology of the larva, and the postlarval development of *Venus striatula*. *Journal of the Marine Biological Association of the United Kingdom*, **42**: 419-433.
- Bellolio G., Lohrmann K. & Dupré R. 1993.** Larval morphology of the scallop *Argopecten purpuratus* as revealed by scanning electron microscopy. *Veliger*, **36**: 332-342.
- Casse N., Devauchelle N. & Le Pennec M. 1998.** Embryonic shell formation in the scallop *Pecten maximus* (Linnaeus). *Veliger*, **41**: 133-141.
- Eyster L.S. 1983.** Ultrastructure of early embryonic shell formation in the opisthobranch gastropod *Aeolidia papillosa*. *Biological Bulletin*, **165**: 394-408.
- Eyster L.S. & Morse M.P. 1984.** Early shell formation during molluscan embryogenesis with new studies on the surf clam *Spisula solidissima*. *American Zoologist*, **24**: 871-882.
- Frenkiel L. & Mouëza M. 1979.** Développement larvaire de deux Tellinacea, *Scrobicularia plana* (Semelidae) et *Donax vitatus* (Donacidae). *Marine Biology*, **55**: 187-195.
- Gibbons M.C. & Castagna M. 1984.** Serotonin as an inducer for spawning in six bivalve species. *Aquaculture*, **40**: 189-191
- Giribet G. & Wheeler W.C. 2002.** On bivalve phylogeny: a high-level analysis of the Bivalvia (Mollusca) based on combined morphology and DNA sequence data. *Invertebrate Biology*, **121**: 271-324.
- Gros O., Frenkiel L. & Mouëza M. 1997.** Embryonic, larval, and post-larval development in the symbiotic clam, *Codakia orbicularis* (Bivalvia : Lucinidae). *Invertebrate Biology*, **116**: 86-101.
- Gros O., Duplessis M.R. & Felbeck H. 1999.** Embryonic development and endosymbiont transmission mode in the symbiotic clam *Lucinoma aequizonata* (Bivalvia : Lucinidae). *Invertebrate Reproduction and Development*, **36**: 93-103.
- Hodgson C.A. & Burke R.D. 1988.** Development and larval morphology of the spiny scallop *Chlamys hastata*. *Biological Bulletin*, **174**: 303-318.
- Kniprath E. 1980.** Larval development of the shell and the shell gland in *Mytilus* (Bivalvia). *Wilhelm Roux's Archives of Developmental Biology*, **188**: 201-204.
- Loosanoff V. & Davis H.C. 1963.** Rearing of bivalve larvae. *Advances in Marine Biology*, **1**: 1-136.
- Loosanoff V., Davis H.C. & Chanley P.E. 1966.** Dimensions and shapes of larvae of some marine bivalve mollusks. *Malacologia*, **4**: 351-435.
- Matsutani T. & Nomura T. 1982.** Induction of spawning by serotonin in the scallop, *Patinopecten yessoensis* (SAY). *Marine Biology Letters*, **3**: 353-358.
- Mouëza M., Gros O. & Frenkiel L. 1999.** Embryonic, larval, and post-larval development of the tropical clam *Anomalocardia brasiliensis* (Mollusca : Bivalvia, Veneridae). *Journal of Molluscan Studies*, **65**: 73-88.
- Mouëza M., Gros O. & Frenkiel L. 2006.** Shell-field differentiation and shell formation in the tropical species *Chione cancellata* (Bivalvia : Veneridae): an ultrastructural analysis. *Invertebrate Biology*, **125**: 21-33.
- Sastry A.N. 1979.** Pelecypoda (excluding Ostreidae). In: *Reproduction of Marine Invertebrates*, vol. 5 *Molluscs. Pelecypods and lesser classes* (A.C. Giese & J.S. Pearse, eds), pp. 113-292. Academic Press, New York.
- Waller T.R. 1981.** Functional morphology and development of veliger larvae of the european oyster *Ostrea edulis* Linné. *Smithsonian Contributions to Zoology*, **328**: 1-70.
- Warmke G.L. & Abbott R.T. 1962.** *Caribbean seashells*. Livingston Narberth, 348 pp.
- Zardus J.D. & Morse M.P. 1998.** Embryogenesis, morphology and ultrastructure of the pericalymma larva of *Acila castrensis* (Bivalvia: Protobranchia: Nuculoida). *Invertebrate Biology*, **117**: 245-252.